Glycoconj J (2008) 25:633–646
DOI 10.1007/s10719-008-9115-y

Versatile strategy for the synthesis of biotin-labelled glycans, their immobilization to establish a bioactive surface and interaction studies with a lectin on a biochip

F. Javier Muñoz · Ángel Rumbero · José V. Sinisterra · J. Ignacio Santos · Sabine André · Hans-J. Gabius · Jesús Jiménez-Barbero · María J. Hernáiz

Received: 2 December 2007 / Revised: 25 January 2008 / Accepted: 28 January 2008 / Published online: 18 March 2008

Abstract The emerging role of glycans as versatile biochemical signals in diverse aspects of cellular sociology calls for establishment of sensitive methods to monitor carbohydrate recognition by receptors such as lectins. Most of these techniques involve the immobilization of one of the binding partners on a surface, *e.g.* atomic force microscopy, glycan array and Surface Plasmon Resonance (SPR), hereby simulating cell surface presentation. Here, we report the synthesis of fluorescent glycoconjugates, with a functionalization strategy which avoids the frequently occurring ring opening at the reducing end for further immobilization on a surface or derivatization with biotin. In order to improve the versatility of these derivatized glycans for biological studies, a new approach for the synthesis of biotinylated and fluorescent glycans has also been realized. Finally, to illustrate their usefulness the neoglycoconjugates were immobilized on different surfaces, and the interaction analysis with a model lectin, the toxin from mistletoe, proved them to act as potent ligands, underscoring the merit of the presented synthetic approach.

Keywords Glycan labelling · Carbohydrate-lectin interactions · Immobilization of glycans · SPR · NMR · Molecular recognition

Introduction

The emerging role of glycans as functional signals in biological information transfer within the cell and at the cell

Electronic supplementary material The online version of this article (doi:10.1007/s10719-008-9115-y) contains supplementary material, which is available to authorized users.

F. J. Muñoz · J. V. Sinisterra · M. J. Hernáiz
Grupo de Biotransformaciones, Departamento de Química Orgánica y Farmacéutica, Facultad de Farmacia, Universidad Complutense de Madrid (UCM), Pz/ Ramón y Cajal s/n., 28040 Madrid, Spain

Á. Rumbero
Departamento de Química Orgánica, Facultad de Químicas, Universidad Autónoma (UAM), 28049 Cantoblanco, Madrid, Spain

J. V. Sinisterra
Servicio de Biotransformaciones Industriales, Parque Científico de Madrid, Tres Cantos, 28760 Madrid, Spain

J. I. Santos · J. Jiménez-Barbero
Departamento de Ciencia de Proteínas, Centro de Investigaciones Biológicas, CIB-CSIC, Ramiro de Maeztu 9, 28040 Madrid, Spain

S. André · H.-J. Gabius
Institut für Physiologische Chemie, Tierärztliche Fakultät, Ludwig-Maximilians-Universität München, Veterinärstr. 13, 80539 München, Germany

M. J. Hernáiz (✉)
Servicio de Interacciones Biomoleculares, Parque Científico de Madrid, Facultad de Farmacia, Universidad Complutense, Pz/ Ramón y Cajal s/n., 28040 Madrid, Spain
e-mail: mjhernai@farm.ucm.es

surface attracts increasing attention to the study of cellular glycoconjugates [1–5]. In fact, even clinically relevant processes such as the inflammatory cascade or growth regulation of malignant cells by a tumor suppressor are regulated by carbohydrate-protein (lectin) interactions, and even subtle structural modifications in the glycan chains can markedly modulate binding affinities [6–9]. Reflecting the increasing understanding of the biological relevance of glycans, a series of analytical procedures such as atomic force microscopy, microarrays and SPR have been adapted to study quantitative aspects of recognition of glycan determinants by lectins [10–14]. In chemical terms, the glycans generally are required to be immobilized on a surface for enabling their presentation to receptors.

A common approach for glycan derivatization is to generate amine reactive compounds by conversion of free glycans into glycosylamines [15–17]. However, these glycan derivatives are generally unstable so that they are recovered in poor yields, are readily hydrolysed, and often afford undesirable side products. Thus, alternatives warrant to be explored.

Within this area, it is well established that free reducing end glycans readily react, by reductive amination, with primary aryl amine reagents, such as the fluorescent 2-aminopyridine [18, 19] or 2,6-diaminopyridine [20–22] moieties. Of note, for the first molecule, the lack of an additional primary amino group precludes further derivatization of the obtained molecule, for instance, by biotinylation or by covalent attachment to solid supports. Regarding structural integrity of the glycan both methods will affect the structure and therefore may influence their binding properties to lectins. Obviously, it will be desirable to develop strategies maintaining the structural integrity.

Toward this end, the work presented herein describes a general strategy for the synthesis of new and properly functionalized glycoconjugates with a fluorescent tag that can be further used as tools for the study of carbohydrate-protein and carbohydrate-carbohydrate interactions. As model, fluorescent labelling of the disaccharide lactose was performed so that the resulting product can be detected by UV-visible or fluorescence spectroscopy, can be biotinylated and covalently attached to a sensor-chip surface. It is demonstrated that the conformational properties of the synthetic derivatives equal the properties of unsubstituted lactose. The same holds true for the bioactivity as ligand tested with a plant toxin, the agglutinin from *Viscum album* (VAA) [23].

Materials and methods

Chemicals and other reagents

All commercial products were used without any further purification step. TLC was used to follow the course of the reactions on Kieselgel plates 60 F_{254} (SDS). Product detection on TLC plates was carried out under UV-lamp light or with 10% H_2SO_4 in MeOH and heating. Column chromatography was carried out, if necessary, on silicagel 60, AC, 40–63 μm (SDS). Sensor chips and solutions used for the SPR assays were purchased from BIAcore. Neutravidin was obtained from Pierce. UV-visible spectra were recorded in a UV-2401 PC Shimadzu. Elemental analysis and mass spectrometry were carried out by the Support Services (CAI) of the UCM. NMR spectra were recorded on Bruker 250, 300, and 500 MHz equipments. Samples were dissolved in the appropriate deuterated solvent ($CDCl_3$, DMSO-d_8 and D_2O), and chemical shifts (δ) are expressed in parts per million (ppm). If necessary for the correct assignment, COSY and ^1H-^{13}C heteronuclear experiments (HMQC and HMBC) were carried out. The lectin from mistletoe (VAA) was purified from extracts of dried leaves by affinity chromatography on lactosylated Sepharose 4B obtained by divinyl sulfone activation and ligand coupling as crucial step and assays to ascertain purity and activity were run by one- and two-dimensional gel electrophoresis and gel filtration or haemagglutination and solid-phase/cell binding [23, 24].

Experimental procedures

Synthesis of compounds **1** to **3** was carried out as described previously and the references given therein [25].

Synthesis of 2-oxoethyl-(2,3,4,6-tetraacetyl-β-D-galactopyranosyl)-(1→4)-2,3,6-triacetyl-β-D-glucopyranoside (**4**)

One gram (1.48 mmol) of **3** was dissolved in 50 ml CH_2Cl_2 anhydrous at −78°C and ozone was introduced in constant flow. After 40 min excess of ozone was removed with a constant flow of argon for 5 min, and an excess of $(CH_3)_2S$ (2 mmol). When reaction lost its blue colour, cooling bath was removed and organic solvent was then evaporated. Purification of the final product was carried by column chromatography, (hexane/EtOAc 1:2) yielding a white solid **4** in 75% yield.

^1H-NMR (250 MHz, $CDCl_3$): 9.65 (dd, 1H, J=1.43, J=0.77, H-1), 5.35 (dd, 1H, J=3.3, J=2.5 Hz, H-4″), 5.22 (t, 1H, J=9.3 Hz, H-3′), 5.11 (dd, 1H, J=10.4, J=7.8 Hz, H-2″), 5.00 (dd, 1H, J=9.4, J=7.8, Hz, H-2′), 4.96 (dd, 1H, J=10.3, J=6.8 Hz, H-3″), 4.55 (d, 1H, J=7.9 Hz, H-1′), 4.49 (d, 1H, J=7.8 Hz, H-1″), 4.47 (dd, 1H, J=12.0, J=2.2 Hz, H-6′a), 4.26 (dd, 1H, J=16.0, J=0.8, H-2a), 4.17 (d, 1H, J=15.0, J=0.8, H-2b), 4.12 (dd, 1H, J=11.9, J=2.4 Hz, H-6″a), 4.08 (dd, 1H, J=12.1, J=5.6 Hz, H-6′b), 4.06 (dd, 1H, J=11.9, J=5.7 Hz, H-6″b), 3.87 (t, J=6.8 Hz, H-5″), 3.81 (t, 1H, J=9.4, H-4′), 3.62 (m, 1H, H-5′), 2.16–

1.97 (21H, CH_3CO). ^{13}C-NMR (63 MHz, $CDCl_3$): 200.04 (C-1), 170.33–169.03 (7-COO-), 101.00 (C-1″), 100.70 (C-1′), 76.10 (C-4′), 74.21 (C-1), 72.80 (C-5′), 72.36 (C-3′), 71.10 (C-2′), 70.83 (C-3″), 70.60 (C-5″), 68.94 (C-2″), 66.48 (C-4″), 61.58 (C-6′), 60.70 (C-6″), 20.72–20.46 (7-CH_3CO). Analysis calculated for $C_{28}H_{38}O_{19}$: C, 49.56%; H, 5.64%. Found: C, 49.57%; H, 5.63%. ESI-MS: [M + Na] calcd., 701.2; found, 701.0.

Synthesis of 2-bromoethyl-(2,3,4,6-tetraacetyl-β-D-galactopyranosyl)-(1→4)-2,3,6-triacetyl-β-D-glucopyranoside (**5**)

To a solution of 500 mg (0.74 mmol) of octaacetyl lactose in 2 ml of anhydrous CH_2Cl_2 at 0°C (ice-water bath) was added 63 μl (0.89 mmol) of 2-bromoethanol, and the reaction mixture was stirred under argon atmosphere. After 30 min, 600 μl (3.70 mmol) of $BF_3°(EtO)_2$ were dropped over the mixture at 0°C for 1 h, afterwards the cooling bath was removed and stirred overnight at room temperature. Reaction mixture was finally added over a stirring ice-water bath. Aqueous fraction was extracted with CH_2Cl_2. The organic phase was washed with water, neutralized with $NaHCO_3$ and then again with water. Afterwards, the organic phase was dried with Na_2SO_4 and solvent was removed. Compound 5 was purified by column chromatography (hexane/EtOAc 1:1). Yield, 40%.

^{1}H-NMR (300 MHz, $CDCl_3$): 5.35 (dd, 1H, *J*=3.3, *J*=2.8 Hz, H-4″), 5.14 (t, 1H, *J*=9.8 Hz, H-3′), 5.03 (dd, 1H, *J*=9.8, *J*=7.8 Hz, H-2″), 4.95 (dd, 1H, *J*=9.8, *J*=3.3 Hz, H-3″), 4.85 (dd, 1H, *J*=9.8, *J*=7.8, Hz, H-2′), 4.43 (d, 1H, *J*=7.8 Hz, H-1′), 4.41 (d, 1H, *J*=7.8 Hz, H-1″), 4.42 (dd, 1H, *J*=11.9, *J*=2.4 Hz, H-6′a), 4.13 (dd, 1H, *J*=11.9, *J*=2.4 Hz, H-6″a), 4.06 (dd, 1H, *J*=11.9, *J*=5.6 Hz, H-6″b), 4.02 (dd, 1H, *J*=11.9, *J*=5.6 Hz, H-6′b), 3.85 (m, 1H, H-5″), 3.74 (t, 1H, *J*=9.8, H-4′), 3.73 (t, 2H, *J*=6.8 Hz, H-1), 3.55 (m, 1H, H-5′), 3.37 (t, 2H, *J*=6.8 Hz, H-2), 2.1–1.9 (21H, CH_3CO). ^{13}C-NMR (63 MHz, $CDCl_3$): 170.76–169.49 (7-COO-), 101.45 (C-1″), 101.45 (C-1′), 76.55 (C-4′), 73.08 (C-5′), 72.92 (C-3′), 71.73 (C-2′), 71.33 (C-3″), 71.02 (C-5″), 70.19 (C-1), 69.42 (C-2″), 66.96 (C-4″), 62.22 (C-6′), 61.18 (C-6″), 30.33 (C-2), 21.29–20.94 (7-CH_3CO). Analysis calculated for $C_{28}H_{39}BrO_{18}$: C, 45.23%; H, 5.29%. Found: C, 45.26%; H, 5.28%. FAB-MS: [M + Na] calcd., 765.1300; found, 765.1297.

Synthesis of 2-iodoethyl-(2,3,4,6-tetraacetyl-β-D-galactopyranosyl)-(1→4)-2,3,6-triacetyl-β-D-glucopyranoside (**6**)

To a solution of 250 mg (0.34 mmol) of compound **5** in 25 ml of acetone highly pure, 1.4 g (9.36 mmol) of NaI were added. The mixture was stirred for 3 h at reflux temperature. When reaction was completed, solvent was removed and the solid substance was redissolved in EtOAc and washed gently with water. Organic phase was then collected, dried with Na_2SO_4, filtered and the solvent removed. Compound **6** is obtained as a yellow solid in quantitative yield.

^{1}H-NMR (300 MHz, $CDCl_3$): 5.37 (dd, 1H, *J*=3.3, *J*=2.8 Hz, H-4″), 5.22 (t, 1H, *J*=9.8 Hz, H-3′), 5.13 (dd, 1H, *J*=9.8, *J*=7.8 Hz, H-2″), 4.97 (dd, 1H, *J*=9.8, *J*=3.3 Hz, H-3″), 4.92 (dd, 1H, *J*=9.8, *J*=7.8, Hz, H-2′), 4.54 (d, 1H, *J*=7.8 Hz, H-1′), 4.49 (d, 1H, *J*=7.8 Hz, H-1″), 4.45 (dd, 1H, *J*=11.9, *J*=2.4 Hz, H-6′a), 4.15 (dd, 1H, *J*=11.9, *J*=2.4 Hz, H-6″a), 4.08 (dd, 1H, *J*=11.9, *J*=5.6 Hz, H-6″b), 4.05 (dd, 1H, *J*=11.9, *J*=5.6 Hz, H-6′b), 3.80 (m, 1H, H-5″), 3.75 (t, *J*=7.2 Hz, H-1), 3.71 (t, 1H, *J*=9.8, H-4′), 3.63 (ddd, 1H, *J*=9.8, *J*=5.0, *J*=2.0, H-5′), 3.24 (t, 2H, *J*=7.2 Hz, H-2), 2.1–1.9 (21H, CH_3CO). ^{13}C-NMR (63 MHz, $CDCl_3$): 170.80–169.51 (7-COO-), 101.48 (C-1″), 100.93 (C-1′), 76.58 (C-4′), 73.09 (C-5′), 72.98 (C-3′), 71.75 (C-2′), 71.34 (C-3″), 71.04 (C-5″), 70.91 (C-1), 69.43 (C-2″), 66.95 (C-4″), 62.22 (C-6′), 61.18 (C-6″), 2.63 (C-2), 21.33–20.95 (7-CH_3CO). Analysis calculated for $C_{28}H_{39}IO_{18}$: C, 45.54%; H, 4.97%. Found: C, 45.52%; H, 4.96%. FAB-MS: [M + Na] calcd., 813.1200; found, 813.1780.

Synthesis of 2-[2′-(6′-aminopyridyl)amino]ethyl-(2,3,4,6-tetraacetyl-β-D-galactopyranosyl)-(1→4)-2,3,6-triacetyl-β-D-glucopyranoside (**7**)

Method 1 To a solution of 100 mg (0.15 mmol) of aldehyde lactoside 4 in 5 ml of dry MeOH was added 80 mg (0.74 mmol) of 2,6-diaminopyridin (DP) and 20 μl of AcOH, and the reaction mixture was stirred at room temperature under argon atmosphere. After 2 h, aldehyde derivative **4** reacted completely as observed by TLC (CH_2Cl_2/MeOH 12:1), and 18 mg (0.30 mmol) of $NaBH_3CN$ were added and the mixture was further stirred for 18 h at room temperature. Solvent was then evaporated and EtOAc was added to the residue and quenched with brine and water. The organic phase was dried (Na_2SO_4), filtered and the solvent removed with a vacuum pump. Product **7** was further purified by column chromatography (CH_2Cl_2/MeOH 12:1) and isolated in a 50% of yield.

Method 2 To a solution of 100 mg (0.13 mmol) of compound 6 in 5 ml of anhydrous toluene, 28 mg (0.26 mmol) of DP were added, and the reaction mixture was stirred under argon atmosphere, at reflux temperature until no further conversion of substrates to products was observed by TLC (CH_2Cl_2/MeOH 20:1). Product **7** was purified by column chromatography (CH_2Cl_2/MeOH 20:1) and isolated in a 40% of yield.

Method 3 To a solution of 100 mg (0.13 mmol) of compound **6** in anhydrous acetonitrile 5 ml, 14 mg

(0.13 mmol) of DP, and 23 mg (0.20 mmol) of KF/Celite (50% weight) were added. The reaction mixture was stirred under argon atmosphere, at 85°C. After 18 h, reaction was filtered over Celite, and solvent was removed in vacuum. Product **7** was further purified by chromatography column (CH_2Cl_2/MeOH 20:1) and isolated in a 75% of yield.

^{1}H-NMR (300 MHz, $CDCl_3$): 7.11 (t, 1H, *J*=8.8 Hz, H-4), 5.75 (d, 1H, *J*=8.8 Hz, H-3), 5.68 (d, 1H, *J*=8.9 Hz, H-5), 5.28 (dd, 1H, *J*=3.3, *J*=2.8 Hz, H-4″), 5.10 (t, 1H, *J*= 9.2 Hz, H-3′), 5.03 (dd, 1H, *J*=9.2, *J*=7.8 Hz, H-2″), 4.90 (dd, 1H, *J*=9.2, *J*=3.3 Hz, H-3″), 4.85 (dd, 1H, *J*=9.2, *J*= 7.8 Hz, H-2′), 4,6 (t, 1H, NH), 4.48 (d, 1H, *J*=7.9 Hz, H-1′), 4.42 (d, 1H, *J*=7.8, H-1″), 4.42 (dd, 1H, *J*=11.9, *J*= 2.4 Hz, 6′a), 4.20 (sw, 2H, NH_2), 4.08 (dd, 1H, *J*=11.9, *J*= 2.4 Hz, H-6″a), 4.02 (dd, 1H, *J*=11.9, *J*=5.6 Hz, H-6′b), 4.01 (dd, 1H, *J*=11.9, *J*=5.6 Hz, H-6″b), 3.80 (m, 1H, H-5″), 3.73 (t, 1H, *J*=9.2, H-4′), 3.72 (t, 2H, *J*=6.8 Hz, H-8), 3.57 (m, 1H, H-5′), 3.35 (t, 2H, *J*=6.8 Hz, H-7), 1.9–2.01 (21H, CH_3CO). ^{13}C-NMR (63 MHz, $CDCl_3$): 170.53–169.04 (7-COO-), 157.37 (C-2), 157.12 (C-6), 139.77 (C-4), 101.07 (C-1″), 100.77 (C-1′), 96.65 (C-3), 95.85 (C-5), 76.26 (C-4′), 72.75 (C-5′), 72.68 (C-3′), 71.67 (C-2′), 70.96 (C-3″), 70.69 (C-5″), 69.76 (C-8), 69.11 (C-2″), 66.60 (C-4″), 62.09 (C-6′), 61.84 (C-6″), 41.73 (C-7), 20.83–20.61 (7CH_3CO).Analysis calculated for $C_{33}H_{45}N_3O_{18}$: C, 51.36%; H, 5.88%; N, 5.44%. Found: C, 51.30%; H, 5.88%; N, 5.49%. FAB-MS: [M + H] calcd., 772.2771; found, 772.2781.

Synthesis of 2-[2′-(6′-aminopyridyl)amino]ethyl-β-D-galactopyranosyl-(1→4)-β-D-glucopyranoside (Lact-DP) (**8**)

To a solution of compound 7 in MeOH were added catalytic amounts of MeONa. The reaction mixture was stirred at room temperature until full conversion of the acetylated compound was observed by TLC (2-propanol: nitromethane:water, 10:9:2). Reaction mixture was then neutralized with Amberlite-IR 120 and filtered. The filtrate was collected and the solvent was removed. Compound 8 (Lact-DP) was obtained in quantitative yield.

^{1}H-NMR (500 MHz, D_2O): 7.20 (t, 1H, *J*=8.8 Hz, H-4), 5.65 (d, 1H, *J*=8.8 Hz, H-3), 5.83 (d, 1H, *J*=8.9 Hz, H-5), 4.32 (d, 1H, *J*=7.8 Hz, H-1′), 4.27 (d, 1H, *J*=7.8, H-1″), 3.75 (t, 2H, *J*=6.8 Hz, H-8), 4.0–3.3 (12H, lactose ring), 3.18 (t, 2H, *J*=6.8 Hz, H-7). ^{13}C-NMR (125 MHz, D_2O): 163.15 (C-2), 158.64 (C-6), 140.86 (C-4), 106.06 (C-3), 103.93 (C-5), 103.34 (C-1″), 102.67 (C-1′), 78.74 (C-4′), 75.75 (C-5′), 75.18 (C-3′), 74.73 (C-2′), 73.26 (C-3″), 72.93 (C-5″), 71.36 (C-2″), 69.20 (C-8), 68.96 (C-4″), 61.42 (C-6′), 60.46 (C-6″), 41.76 (C-7). Analysis calculated for $C_{19}H_{31}N_3O_{11}$: C, 47.79%; H, 6.54%; N, 8.80%. Found: C, 47.78%; H, 6.55%; N, 8.77%. ESI-MS: [M + Na] calcd., 500.2; found, 499.9.

Synthesis of *N*-(6-aminopyridin-2-yl)-biotin (DPB) (10).

One milliliter of oxalyl chloride was dropped over 200 g (0.82 mmol) of biotin. Reaction mixture was stirred at room temperature until complete dissolution of the biotin. Solvent was removed under vacuum and washed with toluene. Compound 9 was obtained as a yellow wax in quantitative yield.

0.29-g (2.66 mmol) of DP were dissolved in 10 ml of CH_2Cl_2 anhydrous and 1 ml of NEt_3 was added to the solution and stirred at 0°C. Then 0.35 g (1.33 mmol) of **9** were solved in 15 ml of CH_2Cl_2 anhydrous and 2 ml of DMF and added to the reaction mixture. After few minutes a precipitate was formed, then filtered and washed with acetone. Final product was obtained in 90% yield.

Characterization data agree with those described in the literature: Rothenberg *et al*. [20].

Synthesis of 2-[2′-(6′-biotinamido-pyridyl)amino]ethyl-*O*-(2,3,4,6-tetraacetyl-β-D-galactopyranosyl)-(1→4)-2,3,6-triacetyl-β-D-glucopyranoside (11)

To a solution of 40 mg (0.06 mmol) of aldehyde lactoside **4** in 3 ml of anhydrous MeOH was added 95 mg (0.28 mmol) of DPB, DMF until complete solubilization of DPB (0.3 ml) and 10 μl of AcOH, and the reaction mixture was stirred at room temperature under N_2 atmosphere. After 5 h of reaction, 7 mg (0.11 mmol) of $NaBH_3CN$ were added and the mixture was further stirred for 18 h at room temperature. Solvent was then evaporated and EtOAc was added to the residue and solid eliminated by filtration. The filtered material was then washed with brine and after with water. The organic phase was dried (Na_2SO_4), filtered and concentrated in vacuum. Product 11 was further purified by column chromatography (CH_2Cl_2/MeOH 12:1) and isolated in a 40% of yield.

^{1}H-NMR (500 MHz, $CDCl_3$): 7.45 (t, 1H, *J*=8.0 Hz, H-4′), 6.26 (d, 1H, *J*=8.0 Hz, H-3′), 6.12 (d, 1H, *J*=8.0 Hz, H-5′), 5.36 (dd, 1H, *J*=3.3, *J*=2.8 Hz, H-4‴), 5.20 (t, 1H, *J*=9.2 Hz, H-3″), 5.09 (t, 1H, *J*=9.2, H-2‴), 4.92 (dd, 1H, *J*=9.2, *J*=3.3 Hz, H-3‴), 4.92 (t, 1H, *J*=9.2 Hz, H-2″), 4.58 (d, 1H, *J*=7.8 Hz, H-1″), 4.56 (dd, 1H, *J*=11.9, *J*= 2.4 Hz, 6″a), 4.53 (d, 1H, *J*=7.8, H-1‴), 4.45 (m, 1H, H-6a), 4.23 (m, 1H, H-3a), 4.16 (dd, 1H, *J*=11.9, *J*=5.6 Hz, H-6″b), 4.15 (dd, 1H, *J*=11.9, *J*=2.4 Hz, H-6‴a), 4.10 (dd, 1H, *J*=11.9, *J*=5.6 Hz, H-6‴b), 3.89 (t, 2H, *J*=6.8 Hz, H-8′), 3.86 (t, 1H, *J*=9.2, H-4″),3.85 (m, 1H, H-5‴), 3.69 (m, 1H, H-5″), 3.37 (t, 2H, *J*=6.8 Hz, H-7′), 3.08 (m, 1H, H-4), 2.91 (dd, 1H, *J*=12.9 Hz, *J*=4.8 Hz, H-6α), 2.73 (d, 1H, *J*=12.9 Hz, H-6β, 2.40 (t, 2H, *J*=7.5 Hz, H-10), 2.09–1.90

(21H, CH_3CO), 1.78 (m, 2H, H-7), 1.65 (m, 2H, H-9), 1.36 (m, 2H, H-8). ^{13}C-NMR (125 MHz, $CDCl_3$): 170.85–169.51 (7-COO-, C-11), 163.95 (C-2), 157.79 (C-6′), 150.34 (C-2′), 140.35 (C-4′), 104.85 (C-3′), 102.48 (C-5′), 101.48 (C-1‴), 100.35 (C-1″), 76.43 (C-4″), 73.10 (C-5″), 72.00 (C-3″), 71.35 (C-2″), 71.05 (C-5‴), 70.33 (C-8′), 70.05 (C-3‴), 69.56 (C-2‴), 67.05 (C-4‴), 62.85 (C-6″), 62.13 (C-3a), 61.28 (C-6‴), 61.19 (C-6a), 55.68 (C-4), 42.41 (C-7′), 40.96 (C-6), 37.41 (C-10), 30.01 (C-7), 28.39 (C-8), 25.70 (C-9), 21.49–20.95 ($7CH_3CO$). Analysis calculated for $C_{43}H_{59}N_5O_{20}S$: C, 51.75; H, 5.96; N, 7.02; S, 3.21. Found: C, 51.73; H, 5.99; N, 6.97; S, 3.22. FAB-MS: [M + H] calcd., 998.3552; found, 998.3542.

Synthesis of 2-[2′-(6′-biotinamido-pyridyl)amino]ethyl-*O*-β-D-galactopyranosyl-(1→4)-β-D-glucopyranoside (Lact-DPB) (**12**)

The experimental procedure for the synthesis of compound **12**, was exactly the same as described for the synthesis of compound **8**. In this case, compound **12** (Lact-DPB) was obtained in quantitative yield.

^{1}H-NMR (500 MHz, D_2O): 7.42 (t, 1H, *J*=8.0 Hz, H-4′), 6.84 (d, 1H, *J*=8.0 Hz, H-3′), 6.29 (d, 1H, *J*=8.0 Hz, H-5′), 4.43 (dd, 1H, *J*=8.0, *J*=4.8 Hz, H-6a), 4.35 (d, 1H, *J*=7.8 Hz, H-1″), 4.28 (d, 1H, *J*=7.8, H-1‴), 4.25 (m, 1H, H-3a), 3.80 (t, 2H, *J*=6.8 Hz, H-8′), 4.0–3.3 (12H, lactose), 3.30 (t, 2H, *J*=6.8 Hz, H-7′), 3.15 (m, 1H, H-4), 2.82 (dd, 1H, *J*=12.9 Hz, *J*=4.8 Hz, H-6α), 2.60 (d, 1H, *J*=12.9 Hz, H-6β, 2.30 (t, 2H, *J*=7.5 Hz, H-10), 1.57 (m, 2H, H-7), 1.50 (m, 2H, H-9), 1.35 (m, 2H, H-8). ^{13}C-NMR (125 MHz, D_2O): 140.78 (C-4′), 103.36 (C-1‴), 102.69 (C-1″), 78.80 (C-4″), 75.76 (C-5″), 75.18 (C-3″), 74.74 (C-2″), 73.24 (C-3‴), 72.94 (C-5‴), 71.36 (C-2‴), 69.23 (C-8′), 68.96 (C-4‴), 62.45 (C-3a), 61.42 (C-6″), 60.66 (C-6a), 60.20 (C-6‴), 55.68 (C-4), 41.75 (C-6), 40.08 (C-7′), 37.50 (C-10), 28.24 (C-7), 28.03 (C-8), 25.28 (C-9). Analysis calculated for $C_{29}H_{45}N_5O_{13}S$: C, 49.49%; H, 6.45%; N, 9.95%; S, 4.56%. Found: C, 49.50%; H, 6.43; N, 9.99%; S, 4.56%. ESI-MS: [M + H] calcd., 726.8; found, 727.8.

Immobilization procedures

For the immobilization of the fluorescent lactoside **8**, a standard CM-5 chip (BIAcore) was activated by the injection of the amino coupling kit (BIAcore): EDC/NHS, 35 μl, at a flow rate of 5 μl/min, at 28°C, and HBS-P (0.01 M HEPES, 0.15 M NaCl, pH=7.4) as running buffer. At the same conditions of flow and temperature, a solution of 8 (1 mM, 180 μl) in sodium acetate buffer 10 mM, pH 4.0 was injected in three portions, followed by the injection of ethanolamine (1 M, 35 μl) to block any remaining active sites on the dextran matrix. The same procedure of activation with EDC/NHS and blocking with ethanolamine was repeated on the flow cell 2 in order to have a control surface. The final response reached was 30 RU.

For the immobilization of the biotinylated and fluorescent compound **12**, a standard SA chip (BIAcore) was conditioned with the standard procedure (BIAcore). A solution in HBS-P of substituted disaccharide **12** (8 mM, 15 μl) was injected at a flow rate of 2 μl/min, at 28°C, three times until a signal of 60 RU was reached. Another flow cell was treated following the same standard procedure and used as control surface.

For the immobilization of neutravidin (Pierce), a CM-5 chip (BIAcore) was activated by the same standard amino coupling procedure (BIAcore) used for the immobilization of compound **8**. At the same conditions (flow rate, 5 μl/min, 28°C), a solution of neutravidin (0.1 mM, 10 μl) in sodium acetate 10 mM, pH 4.5, was injected the times necessary to reach a response of 2,500 RU. The same procedure was repeated in another flow cell to obtain the same density of neutravidin immobilized on the surface. One of the flow cells was used as negative control. In the other flow cell, the same procedure as that used for the immobilization of compound **12** on the SA chip was performed, reaching a maximum response of 40 RU.

Interaction assays

For the interaction assays, different concentrations (1.2, 3.0, 4.7, 5.9, 11.8 and 17.7 μM) of a solution of VAA in HBS-P buffer were injected (15 μl), at a flow rate of 5 μl/min, at 28°C. Sensorgrams obtained for the interaction of VAA with **8** and **12**, immobilized on the chips described above (CM-5, SA and neutravidin-CM-5), were analyzed and kinetic parameters of the interaction were determined with BIAevaluation software (BIAcore).

Conformational analysis by NMR and molecular recognition studies

For picking up the nuclear Overhauser enhancements (NOEs) in the free state, selective experiments were recorded employing a double pulse field-gradient spin-echo (DPFGSE) module [26]. NOE intensities were normalized with respect to the diagonal peak at zero mixing time. Selective T_1 measurements were performed on the anomeric and several other protons to obtain the above-mentioned values. Experimental NOEs were fitted to a double exponential function, as described [27], $f(t)=p0(e^{-p1t})(1-e^{-p2t})$, where $p0$, $p1$ and $p2$ are adjustable parameters. The initial slope was determined from the first derivative at time $t=0$, $f\ (0)=p0p2$. From the initial slopes, interproton distances were obtained by employing the isolated spin-pair approximation (ISPA).

Saturation transfer difference (STD) experiments [28] were performed without saturation of the residual HDO signal for molar ratios between 20:1 and 50:1 of compound/lectin. A train of Gaussian-shaped pulses of 50 ms each was employed, with a total saturation time of the protein envelope of 2 s and a maximum B1 field strength of 50 Hz. An off-resonance frequency of δ=40 ppm and on-resonance frequencies between δ=−1.0 ppm (protein aliphatic signals region) were applied. In all cases, line broadening of ligand protons was monitored. The STD experiments were repeated twice. Basically, similar results were obtained in both sets. In each case, the intensities were normalized with respect to the highest response, which always corresponded to the Gal H-4 proton.

For the bound ligands, trNOE experiments were performed as described previously [29, 30] with a freshly prepared ligand/lectin, mixture with mixing times of 100, 150 and 200 ms and at an approximately 30:1 molar ratio of ligand/protein. A concentration between 2–3 mM of the ligand was employed in all cases. No purging spin-lock period was employed to remove the NMR signals of the macromolecule background. First, line-broadening of the ligand protons was monitored after addition of the lectin. Strong negative NOE cross-peaks were observed, in contrast to the free state, indicating binding of the sugars to the lectin in the mixture. Its carbohydrate-dependent activity had been tested by solid-phase and cell assays, verifying competitive inhibition of glycoconjugate binding by lactose [24].

Molecular mechanics and dynamics calculations

Molecular mechanics and dynamics calculations for free molecules in the free state were performed using the MAESTRO package and the MM3* force field [31]. Charges were taken from the force field (all-atom charge option) and water solvation was simulated using the generalized Born GB/SA continuum solvent model [32]. The torsion angles Φ are defined as H1Gal–C1Gal–O–C4Glc and Ψ as H4Glc–C4Glc–O–C1Gal. For the pendant chain, Φ *chain* is H1Glc–C1Glc–O–CH_2 and Ψ *chain* is C1Glc–O–CH_2–CH_2. The torsion angle around the C5–C6 linkage (ω) is defined as O5–C5–C6–O6. Two different conformers were considered gt (ω=+60°) and gg (ω=−60°) for the Gal and Glc moieties, respectively. The Φ/Ψ maps computed from the 3 ns MD simulations (1.5 fs integration step, 300 K) were drawn and analysed as described [33, 34]. The numbering is given in the corresponding scheme.

Docking calculations

First, the most stable conformer of **1** (as derived by NMR) was manually docked on the reported structure of VAA (pdb code, 1PUM) by superimposing the terminal Gal residue. Then, different possibilities of arranging the side chain were used as input geometries for AutoDock 3.0 simulations [35] with the multiple Lamarckian Genetic Algorithm. The lectin coordinates were obtained (pdb code, 1PUM) from the Protein Data Bank [36]. Two binding sites are known to be present in this structure and operative in solution albeit with different degree of accessibility, one at Trp38 and a second one at Tyr249 [37]. Thus, the two sites are referred as Trp and Tyr sites, as done previously [37]. Only local searches were performed centered in the two experimental X-ray sites. Grids of probe atom interaction energies and electrostatic potential were generated by the AutoGrid program available in AutoDock 3.0. Grid spacings of 0.6 and 0.375 Å were used for the global and local searches, respectively. For each calculation, 100 docking runs were performed using a population of 200 individuals and an energy evaluation number of 3×10^6.

Results and discussion

Design and synthesis of properly functionalized glycans with a fluorescent tag

For the synthesis of the fluorescently tagged glycans we followed two different strategies. Firstly, applying the methodology of Dasgupta *et al*. [25], per-*O*-acetylated lactose **1** was synthesized, followed by the activation via bromide derivative **2**. Finally, allyl alcohol was bound to the anomeric position in the presence of mercury oxide and mercury bromide. This method yielded the desired β-allyl-lactoside **3**. The major advantage of introducing the allyl chain is that it allows the functionalization of the carbohydrate without impairing its pyranose ring. This is an important prerequisite for ensuing molecular recognition studies.

Then, functionalization of the linker chain was carried out by ozonolysis at −78°C in CH_2Cl_2 to yield glycoside **4** in 75% yield [38]. This aldehyde compound **4** is the starting material for the synthesis of the target fluoresce-tagged and biotinylated fluorescently labeled glycans (Figs. 1 and 5).

Further modification of the carbohydrate required fluorescent labeling of the functionalized lactoside aldehyde, **4**. For this purpose, DP was chosen as the fluorescent tag. In a first approach, due to the expected low reactivity of the aminopyridine derivative, we followed a method described for pyridine derivatives through the formation of stable Schiff bases [39]. This methodology required high temperature (toluene reflux), and for **4**, these extreme conditions led to the formation of a mixture of monomeric, dimeric and trimeric structures, as detected by mass spectrometry (see "Supplementary material").

Based on these results, reductive amination should be carried out at mild conditions, with moderate amount of

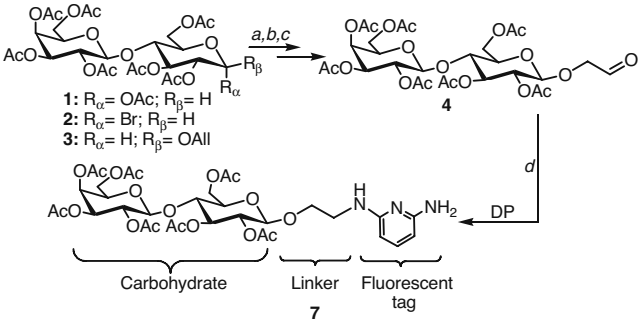

Fig. 1 Synthesis of fluorescent glycan via reductive amination. *a* HBr, CH_2Cl_2. *b* Allyl alcohol, $HgBr_2$, HgO, CH_2Cl_2. *c* O_3, −78°C, CH_2Cl_2. *d* (*1*) DP, MeOH; (*2*) $NaCNBH_3$

reductive reagents such as sodium borohydride derivatives. Therefore, reductive amination of **4** with DP was carried out at rather mild conditions, leading to imine formation in weakly acidic milieu at room temperature, while further reduction with $NaBH_3CN$ led to the labeled product **7**, with 50% yield. When comparing this number with that reported for reductive amination with a monosubstitued pyridine [38], of only 29%, a significant gain was observed. Besides this significant advantage, a complete regioselective control was also achieved by this procedure. With the proper reaction conditions, room temperature and high excess of the amino derivative, the reductive amination took place in only one of the two amino groups of DP. Thus, the desired product, with a linker that avoids the opening of the ring of the carbohydrate at the reducing end, was obtained. Compound **7** also bears a free amino group attached to the pyridine ring, which is the key moiety for further immobilization of these compounds on functionalized surfaces activated by carboxylate groups or for further derivatization (Fig. 2).

The second strategy was carried out with an alternative linker in order to reduce the number of synthetic steps (Fig. 3). In this approach, per-*O*-acetylated lactose was functionalized with 2-bromethanol to produce compound **5**. Then, bromine was exchanged by iodine to improve the properties of the leaving group to yield **6** [40]. This compound **6** was the starting material for a different type of fluorescent labeling of carbohydrates with DP. DP presents a free amino group able to bind to the electrophilic carbon of the new linker chain of **6**. Although the amino group is not a very strong nucleophile, it was shown to be appropriate for the coupling of the fluorescent tag to the glycan. The reaction failed to proceed when it was carried out in DMF as solvent at high temperature, but when toluene was used, we obtained compound **7** in 40% yield. In order to improve the yield, the reaction was carried out in reflux of acetonitrile, with a solid-supported catalyst, *i.e.* KF over Celite. After 18 h, the fluorescent glycan **7** was obtained with 75% yield. Thus, the yields for the synthesis of the fluorescent glycan **7** have been increased from 40% without catalyst to 50% by reductive amination, up to 75%, by using a solid catalyst like KF/Celite [41].

The protected compound **7** was readily deprotected using standard procedures (see "Experimental procedures"). In this way, the fluorescent glycan **8** (Lact-DP) was obtained.

Synthesis of biotinylated fluorescent glycoconjugate

The well-known strong affinity of biotin for avidin/streptavidin (K_D=10^{-15} M) is one of the most preferred ways for the immobilization of biomolecules [20, 42, 43]. Coupling methods typically used for peptide synthesis like 1-ethyl-3-(3-dimethylamino-propyl)carbodiimide (EDC) and *N*-hydroxy-succinimide (NHS) have been reported previously to be an extended procedure for the biotinylation of oligosaccharides [20, 21, 44].

A main problem in the biotinylation of oligosaccharides with the EDC/NHS reagents is the formation of side products, which confound the purification steps with consequently reduced yields. Thus, we decided to explore a new general methodology towards biotinylated glycans exploiting the formation of the biotinyl chloride and further

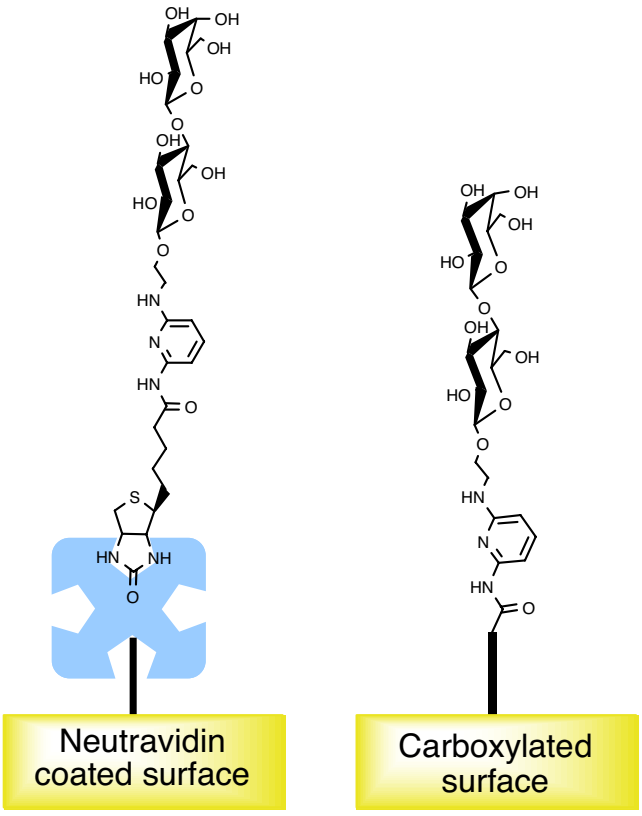

Fig. 2 Immobilization of properly functionalized glycans. The free amino group of the labeled carbohydrates allows the immobilization through coupling to a carboxylated surface. Biotinylated molecules are immobilized by its affinity to streptavidin/neutravidin

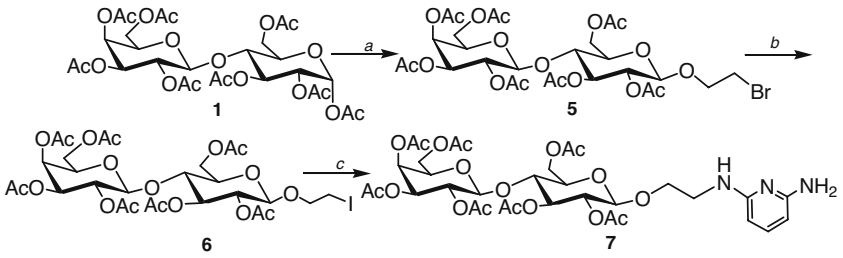

Fig. 3 Synthesis of fluorescent glycan via nucleophile substitution. *a* $BF_3°Et_2O$, Br-ethanol, CH_2Cl_2. *b* NaI, acetone, reflux. *c* DP, toluene, reflux

coupling to DP to obtain a biotinylated fluorescent reagent (DPB) in a convenient step. In order to carry out the amine coupling reaction of the biotin with DP, the activation via oxalyl chloride was performed. As shown in Fig. 4, biotin was activated in quantitative yield to give **9**, and the biotinyl chloride derivative **9** was added to a solution of DP in CH_2Cl_2 in the presence of NEt_3 at 0°C, leading to a solid precipitate few minutes later. Temperature was a key factor for this procedure. When the reaction was carried out at room temperature (25°C), formation of a complex mixture of compounds was observed; in contrast, at 0°C these secondary reactions almost disappeared.

Furthermore, under our reaction conditions, the precipitation of DPB **10** allows its immediate isolation by filtration, representing the main advantage of this procedure. With this methodology we avoided the amido coupling with EDC/NHS which involved complex purification steps and low yields (30–38%) [21]. Thus, DPB was obtained in a rather high overall yield (90%) with a comparatively easy procedure. This new general methodology was applied for the proper functionalization of the previously synthesized lactoside (**7**) with the biotinylated fluorescent tag.

The reaction of functionalized lactoside **4** with the DPB **10** was carried out by reductive amination with $NaBH_3CN$, producing a white compound **11** in 40% yield (Fig. 5). The protected compound **11** was then readily deprotected using standard procedures (see "Experimental procedures"). UV/visual analysis of DPB gave excitation and emission maxima of 341 and 387 nm, respectively (for DPB-oligosaccharide adducts, the corresponding values were 345 and 400 nm) as was described previously by Rothenberg *et al*. [20]. For that reason, we can conclude that the DP derivatization provides fluorescent glycan derivatives for quantification and visualization on a surface such as the specificity studies performed by Xia *et al*. [22].

This approach has led to an *O*-linked labelled glycan, which maintains the ring structure at the reducing end. Alternative approaches have led either to ring-opened labelled structures or to *N*- or *S*-glycosyl analogues attached to a chromophore [45], or to just a linker without additional labelling [44].

Conformational properties of the derivatized glycan in the absence or presence of VAA

The newly synthesized glycans harbor new groups at the reducing end of the Glc moiety. The addition of lipophilic groups may somehow modify the interaction properties of natural lactose and, additionally, the presence of an aromatic ring could also induce conformational changes by intramolecular aromatic-carbohydrate interactions [46]. These interactions have been shown to be of paramount importance for sugar recognition by natural [2, 47] and

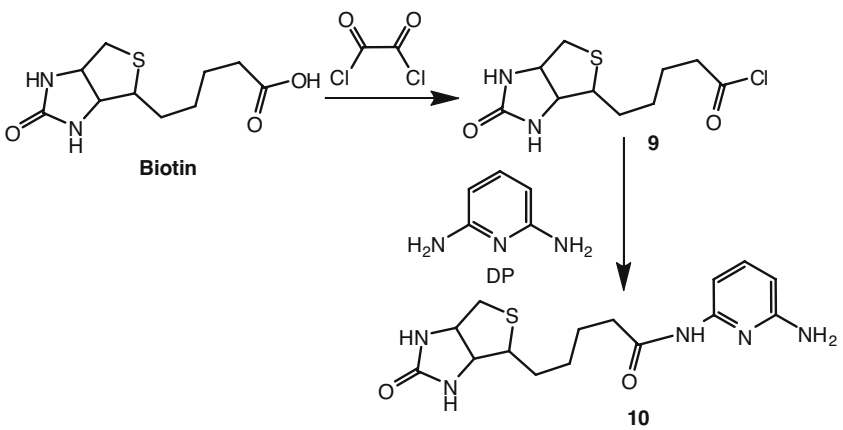

Fig. 4 Synthesis of DPB through the formation of the biotinyl chloride. This methodology requires an easier work-up than the classical EDC/NHS activation

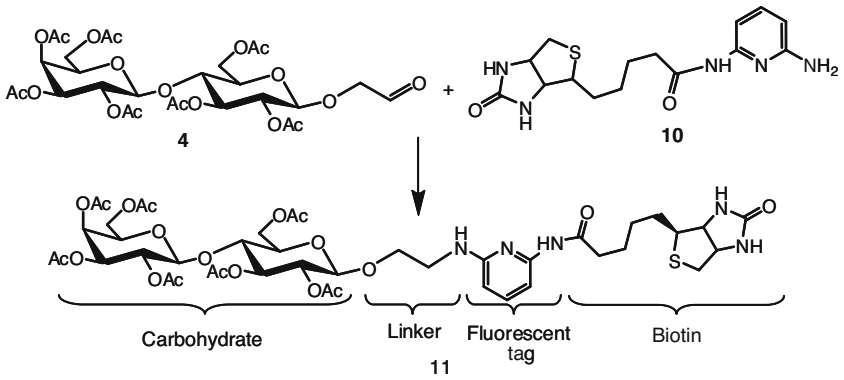

Fig. 5 Synthesis of the biotinylated fluorescent glycans

model receptors [48], especially with galactose as ligand. In solution, such a contact could also be recorded for VAA and galactose derivatives harbouring a lipophilic group showed enhanced affinity [37, 49,–51].

To address the listed issues, the conformational behavior of Lact-DP was analyzed in water solution using a combination of NMR experiments, as well as molecular mechanics and dynamics calculations. The ^{1}H NMR chemical shifts and coupling constants, as obtained at 500 MHz and 300 K, are given in the supporting information. The analysis of the coupling constants permitted to assess that the Glc and Gal rings keep the natural $^{4}C_{1}$(D) conformation. Next, the conformation around the glycosidic linkage was assessed through NOE experiments. Only the expected interresidue GalH1 to GlcH4 (overlapping with GlcH3) and GlcH6 NOEs were observed indicating that LacDP adopts the natural exo-anomeric syn-$\Phi\Psi$ geometry of lactose around the glycosidic linkage [52]. No intramolecular aromatic-sugar NOEs were observed, indicating that no stacking of the aromatic moiety onto the sugar faces takes place. Thus, the pendant DP group stands away from the lactose moiety. A view of the major conformer, which satisfies the experimental NOE data, is given in Fig. 6. Moreover, MD simulations (3 ns, 300 K) were performed. They showed that the lateral chain, although flexible, only accessed a well-defined area of the available conformational space. The obtained conformational maps are also given in the supporting information. In aggregate, the free states of lactose and the synthesized derivative are very similar, if not identical. What happens in the presence of a receptor was studied next by monitoring binding to VAA as model.

The interaction of Lact-DP with VAA was analyzed by NMR to ligand binding by this model lectin. In a first step, STD experiments were carried out. This technique relies on the transfer of saturation from the protein to the ligand and therefore provides information on the proximity of the individual protons of the ligand to the protein surface. As documented for a human lectin and a pentasaccharide recently [53], contact mapping can readily be performed without isotope labelling.

The STD experiments permitted to unambiguously demonstrate that the lectin recognizes Lact-DP. Clear STD signals for the sugar protons in the ligand were observed (Fig. 7). The maximum enhancements were observed for the protons at the Gal moiety, followed by contiguous protons of the Glc part. Small enhancements were even evident at the linker, especially the CH_2 moiety contiguous to the Glc unit, while the DP protons showed moderate enhancements at long saturation times, indicating a minor interaction of this moiety with VAA. Having hereby mapped the contact, we next proceeded to determine conformational properties of the bound ligand.

Toward this aim, trNOE experiments were carried out. As previously shown, for ligands that are not bound tightly and for which exchange between the free and bound states occurs at a reasonably fast rate, trNOE spectroscopy provides an adequate means for determining the conformation of the bound ligand [54, 55].

In the bound state, strong and negative NOE cross-peaks were observed in the presence of the lectin at a 30:1 ligand/receptor molar ratio (Fig. 8). This observation contrasts with findings noted for the free state, for which NOE cross-

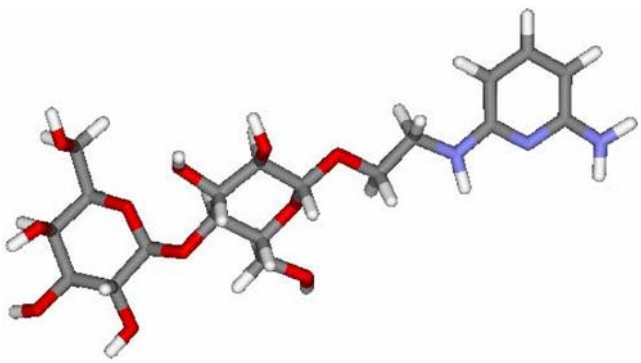

Fig. 6 The major conformation of Lact-DP, as deduced from NMR and MD simulations with the MM3* force field

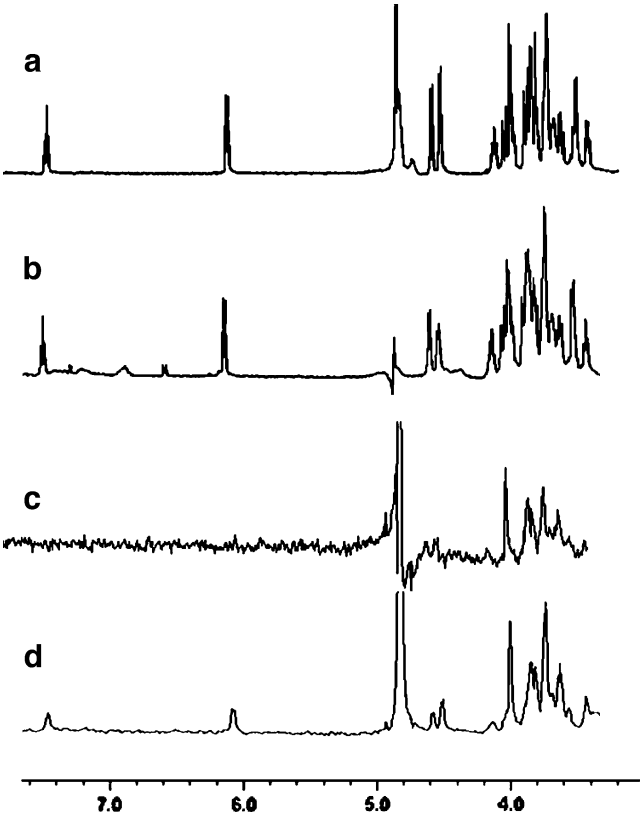

Fig. 7 The interaction of Lact-DP with VAA. **a** The regular 500 MHz 1H NMR spectrum of LacDP at 300 K. **b** The spectrum of Lact-DP in the presence of VAA (30:1). Line broadening is observed, especially in the Gal protons. **c** The STD spectrum (saturation time 600 ms, on resonance irradiation at δ −1 ppm), showing only the Gal protons, especially H2, H3, H4, H5, and H6. Minor transfer to the Glc moiety and no transfer to the 2DP moiety is observed. Increasing the saturation time to 2 s, the Glc protons are also observed, as well as additional saturation transfer to the linker protons and even to the 2DP protons. In any case, the binding epitope clearly belongs to the Gal moiety

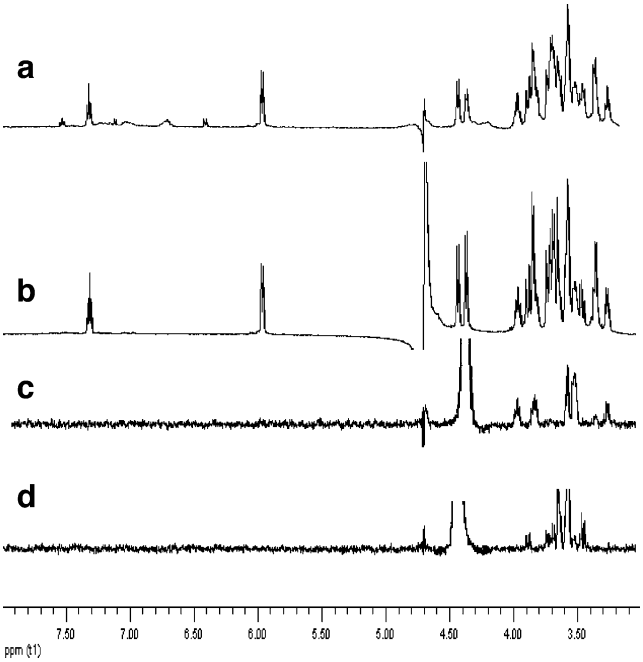

Fig. 8 Key sections of the trNOESY (mixing time, 200 ms) for the Lact-DP/VAA complex (30:1 molar ratio) at 500 MHz and 300 K. Traces **c** and **d** show the negative NOE cross peaks obtained after inversion of the anomeric H-1 Glc and H-1 Gal, respectively. The observed NOEs are basically identical to those observed in the free state (*i.e.*, H1Gal-H4Glc, H1Gal-H6ab Glc, H1Glc-CH2 linker). No NOEs to the aromatic protons are observed. All this information indicates that the disaccharide moiety adopts the regular lactose conformation, with no remote sugar-aromatic contacts. Trace **b** shows the regular 500 MHz 1H NMR spectrum of Lact-DP, while trace **a** shows the spectrum of Lact-DP in the presence of VAA (30:1). Line broadening in observed, especially concerning the Gal protons

peaks were exclusively positive. Thus, as seen in STD spectra, binding of the derivative is not impaired. The analysis of the cross-peaks was performed to determine the experimental proton–proton distances in the bound state. The analysis indicated that basically the free-state conformation of Lact-DP is accommodated into the binding site of VAA, since the cross-peak pattern was identical to that described above for the free glycan.

As final step of this study part, the major conformer, as deduced by NMR, was docked into the VAA binding site using the programme Autodock. The Trp/Tyr binding sites was detected as the major targets by the program, and the bound conformer perfectly adjusted to the 3D-shape of the lectin at these sites (Fig. 9). Of note, when dimeric VAA preferentially binds ligands to the Tyr site in subdomain 2γ due to differences in spatial accessibility [37].

A similar behaviour regarding the major conformer for the lactose moiety as well as the contacts with VAA, as determined by STD, was observed for the biotinylated analogue, Lact-DPB (data in supporting information). As conclusion, no major modifications of the presentation of lactose to the natural receptor take place by attaching through a 2-carbon linker the DP moiety and derivatives

Fig. 9 A 3D model of the complex of VAA (coordinates taken from the Protein Data Bank, code 1PUM) with Lact-DP. Independent AUTODOCK simulations were performed with the Trp38 and Tyr249 binding sites as described in the experimental part. The figure shows the best result for both cases. No contacts between the linker or the 2DP moiety and the protein are observed

thereof and no significant contribution of binding by the linker was picked up. Having herewith demonstrated effective binding, we proceeded to explore multivalency effects by attaching these glycans to surfaces and monitoring the effects by SPR measurements.

Immobilization of fluorescent glycans on a biochip and measurement of their binding affinities to a model lectin by SPR.

SPR, a powerful analytical method to investigate carbohydrate-protein molecular recognition processes in real time requires coating of special sensor chips with a gold sheet inside. Different ways of immobilization are feasible, exploiting an extended dextran matrix functionalized with carboxylic groups or a streptavidin-coated gold surface. The versatile synthetic methodology described above has made it possible to prepare fluorescent glycans that could readily be immobilized on to the surfaces. The fluorescent glycoconjugate **8** (Lact-DP) was covalently immobilized on a sensor chip CM-**5** (carboxymethylated dextran surface, flow cell 1) by amine coupling reaction with EDC and NHS. Immobilization was ascertained by an increase of 50 RU (relative response unit). This relative response is directly proportional to the mass close to the gold surface. An increase of this response means that the injected compound bound to the surface or interacted with the compound immobilized on that surface. After immobilization of Lact-DP **8**, unreacted sites on the sensor surface were blocked with an injection of ethanolamine. As negative control, a second flow cell of the CM-5 sensor chip was treated only with the standard activation and blocking procedures (flow cell 2). The immobilization was also confirmed by the injection of the galactose-binding protein (VAA). The response from the control cell was subtracted from the response in the cell with the immobilized ligand to give a signal (30 RU, relative response units) that was directly proportional to the amount of the bound compound.

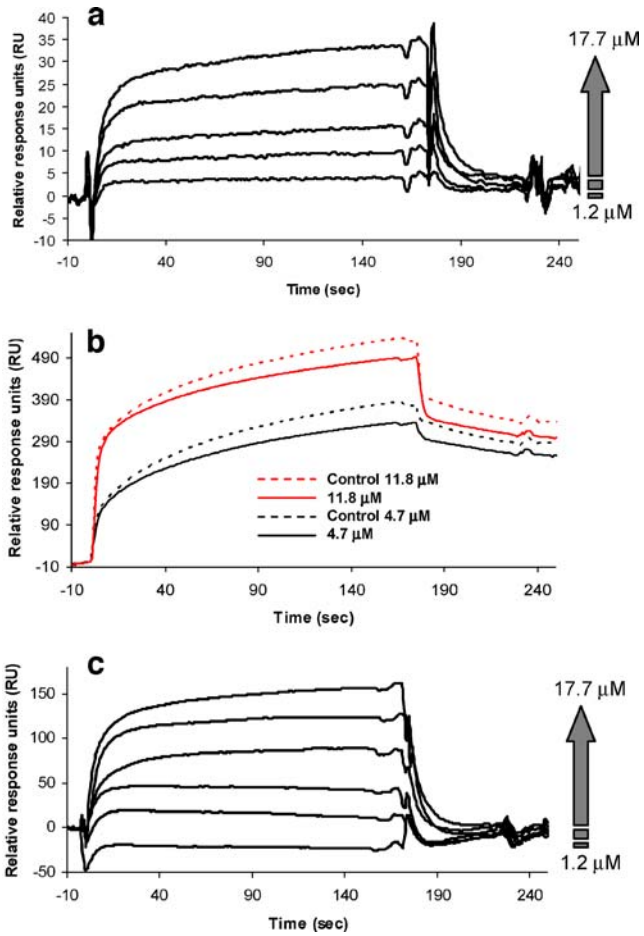

Fig. 10 **a** SPR sensorgrams for the interaction of VAA with immobilized Lact-DP. VAA at different concentrations (1.2–17.7 µM) was flown over a biochip containing immobilized Lact-DP. **b** SPR sensorgrams of VAA interacting with immobilized Lact-DPB on a streptavidin biochip. The interaction with the control cell (streptavidin) is stronger than with Lac-DPB. **c** SPR sensorgrams of VAA interacting with immobilized Lact-DPB on a neutravidin biochip. VAA at different concentrations (1.2–17.7 µM) was passed over a biochip containing immobilized Lact-DP

Table 1 Kinetics of binding of VAA to Lact-DP and Lact-DPB determined by SPR

Compound	k_{on} (M^{-1} s^{-1})	k_{off} (s^{-1})	K_D (µM)
Lac-DP	7.50×103	0.028	37.5
Lac-DPB	1.86×103	0.085	46.0

The interaction of compound **8** (Lact-DP) with VAA was analyzed at different VAA concentrations to allow the determination of rate constants and affinity parameters. Sensorgrams for the binding of VAA to compound **8** (Lact-DP) are shown in Fig. 10a. Both the association and dissociation kinetics fitted a one-site model. The on-rate (k_{on}), off-rate (k_{off}) and dissociation constants for this interaction are given in Table 1.

A relatively fast association phase ($k_{on}= 7.5\times10^2$ M^{-1} s^{-1}) and a gradual dissociation phase (k_{off} =0.028 s^{-1}) are shown in the curves for the binding of VAA and immobilized Lact-DP (Fig. 10a). The binding abilities are characterized by the respective dissociation constants K_D, where $K_D=k_{off}/k_{on}$ (Table 1). A K_D of 37.5 µM was obtained, which is in agreement with previously reported data for the interaction of VAA with lactose [10, 49, 50].

In our application, the streptavidin-coated sensor chip (SA) was used for the immobilization of biotinylated fluorescent glycan **12** and monitored using the SPR technique. The first flow cell of the chip was treated with biotinylated compound **12** until a maximum response of 60 RU was reached, while the second one was used as control cell.

Then, different concentrations of VAA (1.2–17.7 µM) were injected to study the interaction with Lact-DPB 12. However, it was observed that the lectin exhibited stronger

affinity for the streptavidin matrix (control cell) than for the glycan (Fig. 10b). In order to address this problem, neutravidin, a deglycosylated derivative of avidin, was used for affinity assays as alternative. The same density of neutravidin was immobilized on a CM5 BIAcore sensor chip in two different flow cells (~2,400 RU). One of it was used as negative control, and in the other one, Lact-DPB was immobilized (40 RU). Unlike the streptavidin-biotin set-up, neutravidin proved favourable as rather inert matrix, thus allowing to carry out the kinetic study of the interaction by SPR. The binding affinity of Lact-DPB immobilized on the neutravidin-coated matrix to VAA was determined (Fig. 10c). The sensorgrams clearly showed that VAA specifically interacts with 12 (Lact-DPB), while an almost negligible interaction was detected with the reference cell. As in the case of **8** (Lact-DP), the association and dissociation kinetics fitted a one-site model, and the on-rate (k_{on}), off-rate (k_{off}), and dissociation constants for this interaction are given in Table 1. The obtained values for k_{on} (1.86×10^3 M^{-1} s^{-1}), k_{off} (0.085 s^{-1}) and K_D (46.0 μM) for the binding of VAA and immobilized Lact-DPB are in the same range as those obtained for Lact-DP.

According to these results, Lact-DP and Latc-DPB remain bioactive when immobilized on the tested functionalized surfaces.

Conclusion

We have developed an efficient and versatile strategy to synthesize fluorescent and biotin-labeled glycans, which can be immobilized on a biochip and then used as carbohydrate-presenting surface for SPR studies (tested here) or high-throughput screening for novel carbohydrate-binding proteins. To underpin this application, we used assays with a model lectin. The given strategy fulfils three prerequisites favorable for wide application:

1. The ring structure of the reducing end remained unaltered. The linker chain bound to the carbohydrate avoids the opening of the glucose ring after the reductive amination coupling reaction or nucleophile substitution. Furthermore, the linker allows the molecule to be spatially separated from the surface, adding a boon to the consideration of advantages.
2. A fluorescent tag was attached to the structure in order to enable its visual detection and quantification at low concentration ranges for versatile applications. In addition, the free amino group allows its immobilization on carboxylated functionalized surfaces.
3. We have also synthesized functionalized glycans, which allow their immobilization on surfaces by two different approaches. The free amino group is coupled to carboxylated surfaces, and the biotin molecule makes possible its convenient immobilization on popular systems such as streptavidin/neutravidin-coated surfaces.

These fluorescent glycans thus are tools to establish carbohydrate-presenting surfaces or, when conjugated to an inert carrier, neoglycoconjugates for a wide variety of applications [56, 57].

Acknowledgement This work was supported by a Research Project of the MEC (Ministerio de Educación y Ciencia de España, CTQ2006-09052/BQU), a European Project (FP-62003-NMP-SMF-3, proposal 011774-2), an EC Marie Curie Research Training Network grant (MRTN-CT-2005-019561), the research initiative LMU*excellent* and one of the authors (F. Javier Muñoz) thanks the MEC for a Ph.D. grant (MEC-FPU predoctoral fellowship AP2003-4820).

References

1. Reuter, G., Gabius, H.-J.: Eukaryotic glycosylation: whim of nature or multipurpose tool? Cell. Mol. Life Sci. **55**, 368–422 (1999)
2. Bertozzi, C.R., Kiessling, L.L.: Chemical glycobiology. Science **291**, 2357–2369 (2001)
3. Solís, D., Jiménez-Barbero, J., Kaltner, H., Romero, A., Siebert, H.-C., von der Lieth, C.-W., Gabius, H.-J.: Towards defining the role of glycans as hardware in information storage and transfer: basic principles, experimental approaches and recent progress. Cells Tissues Organs **168**, 5–23 (2001)
4. Schmidt, M.A., Riley, L.W., Benz, I.: Sweet new world: glycoproteins in bacterial pathogens. Trends Microbiol. **11**, 554–561 (2003)
5. Gabius, H.-J., Siebert, H.-C., André, S., Jiménez-Barbero, J., Rüdiger, H.: Chemical biology of the sugar code. Chem. Biochem. **5**, 740–764 (2004)
6. Rudd, P.M., Elliot, T., Cresswell, P., Wilson, I.A., Dwek, R.A.: Glycosylation and the immune system. Science **291**, 2370–2376 (2001)
7. Gabius, H.-J.: Cell surface glycans: the why and how of their functionality as biochemical signals in lectin-mediated information transfer. Crit. Rev. Immunol. **26**, 43–80 (2006)
8. André, S., Kožár, T., Schuberth, R., Unverzagt, C., Kojima, S., Gabius, H.-J.: Substitutions in the N-glycan core as regulators of biorecognition: the case of core-fucose and bisecting GlcNAc moieties. Biochemistry **46**, 6984–6995 (2007)
9. André, S., Sanchez-Ruderisch, H., Nakagawa, H., Buchholz, M., Kopitz, J., Forberich, P., Kemmner, W., Böck, C., Deguchi, K., Detjen, K.M., Wiedenmann, B., von Knebel Doeberitz, M., Gress, T.M., Nishimura, S.-I., Rosewicz, S., Gabius, H.-J.: Tumor suppressor p16INK4a modulator of glycomic profile and galectin-1 expression to increase susceptibility to carbohydrate-dependent induction of anoikis in pancreatic carcinoma cells. FEBS J. **274**, 3233–3256 (2007)
10. Dettmann, W., Grandbois, M., André, S., Benoit, M., Wehle, A. K., Kaltner, H., Gabius, H.-J., Gaub, H.E.: Differences in zero-force and force-driven kinetics of ligand dissociation from *b*-galactosidase-specific proteins (plant and animal lectins, immunoglobulin G) monitored by plasmon resonance and dynamic single molecule force microscopy. Arch. Biochem. Biophys. **383**, 157–170 (2000)
11. Schäffer, C., Messner, P.: Glycobiology of surface layer proteins. Biochimie **83**, 591–599 (2001)

12. Hirabayashi, J.: Oligosaccharide microarrays for glycomics. Trends Biotechnol. **21**, 141–143 (2003)
13. Sanchez, J.-F., Lescar, J., Chazalet, V., Audfray, A., Gagnon, J., Alvarez, R., Breton, C., Imberty, A., Mitchell, E.P.: Biochemical and structural analysis of Helix pomatia agglutinin. J. Biol Chem. **281**, 20171–20180 (2005)
14. Shin, S., Park, S., Lee, M.R.: Carbohydrate microarrays: an advanced technology for functional studies of glycans. Chem. Eur. J. **11**, 2894–2901 (2005)
15. Likhosherstov, L.M., Novikova, V.A., Dervitskaya, V.A., Kochetkov, N.K.: A new simple synthesis of amino sugar β-glycosylamines. Carbohydr. Res **146**, c1–c5 (1986)
16. Vetter, D., Gallop, M.A.: Strategies for the synthesis and screening of glycoconjugates. A library of glycosylamines. Bioconjug. Chem. **6**, 316–318 (1995)
17. Hackenberger, C.P.R., O'Reilly, M.K., Imperiali, B.: Improving glycopeptide synthesis: a convenient protocol for the preparation of β-glycosylamines and the synthesis of glycopeptides. J. Org. Chem. **70**, 3574–3578 (2005)
18. Bigge, J.C., Patel, T.P., Bruce, J.A., Goulding, P.N., Charles, S. M., Parekh, R.B.: Nonselective and efficient fluorescent labelling of glycans using 2-amino benzamide and anthranilic acid. Anal. Biochem. **230**, 229–238 (1995)
19. Locke, D., Bevans, C.G., Wang, L.-X., Zhang, Y., Harris, A.L., Lee, Y.C.: Neutral, acidic, and basic derivatives of anthranilamide that confer different formal charge to reducing oligosaccharides. Carbohydr. Res. **339**, 221–231 (2004)
20. Rothenberg, B.E., Hayes, B.H., Toomre, D., Manzi, A.E., Varki, A.: Biotinylated diaminopyridine: an approach to tagging oligosaccharides and exploring their biology. Proc. Natl. Acad. Sci. USA **90**, 11939–11943 (1993)
21. Toomre, D., Varki, A.: Advances in the use of biotinylated diaminopyridine (BAP) as a versatile fluorescent tag for oligosaccharides. Glycobiology **4**, 653–663 (1994)
22. Xia, B., Kawar, Z.S., Ju, T., Alvarez, R.A., Sachdev, G.P., Cummings, R.D.: Versatile fluorescent derivatization of glycans for glycomic analysis. Nat. Methods. **2**, 845–850 (2005)
23. Jiménez, M., Sáiz, J.L., André, S., Gabius, H.-J., Solís, D.: Monomer/dimer equilibrium of the AB-type lectin from mistletoe enables combination of toxin/agglutinin activities in one protein: analysis of native and citraconylated proteins by ultracentrifugation/gel filtration and cell biological consequences of dimer destabilization. Glycobiology **15**, 1386–1395 (2005)
24. André, S., Kaltner, H., Furuike, T., Nishimura, S.-I., Gabius, H.-J.: Persubstituted cyclodextrin-based glycoclusters as inhibitors of protein-carbohydrate recognition using purified plant and mammalian lectins and wild-type and lectin-gene-transfected tumor cells as targets. Bioconjug. Chem. **15**, 87–98 (2004)
25. Dasgupta, F., Anderson, L.: Efficient preparation of allyl 2,3,6,2″,3″,6″-hexa-*O*-benzyl-*b*-lactoside and its use as a glycosyl acceptor for chain extension at O-4″. Carbohydr. Res. **264**, 155–160 (1994)
26. Stott, K., Stonehouse, J., Keeler, J., Hwang, T.L., Shaka, A.J.: Excitation sculpting in high-resolution nuclear magnetic resonance spectroscopy: application to selective NOE experiments.. J. Am. Chem. Soc. **117**, 4199–4200 (1995)
27. Asensio, J.L., Cañada, F.J., Khan, N., Mootoo, D.A., Jiménez-Barbero, J.: Conformational differences between O- and C-glycosides: The alpha-O-Man-(1(1)-beta-Gal/alpha-C-Man-(1(1)-(-Gal case-A decisive demonstration of the importance of the exo-anomeric effect on the conformation of glycosides. Chem. Eur. J. **6**, 1035–1041 (2000)
28. Mayer, M., Meyer, B.: Group epitope mapping by saturation transfer difference NMR to identify segments of a ligand in direct contact with a protein receptor. J. Am. Chem. Soc. **123**, 6108–6117 (2001)
29. Asensio, J.L., Espinosa, J.F., Dietrich, H., Cañada, F.J., Schmidt, R.R., Martin-Lomas, M., André, S., Gabius, H.-J., Jiménez-Barbero, J.: Bovineheart galectin-1 selects a unique (Syn) conformation of C-lactose, a flexible lactose analogue. J. Am. Chem. Soc. **121**, 8995–9000 (1999)
30. Asensio, J.L., Martin-Pastor, M., Jiménez-Barbero, J.: The use of cvff and cff91 force-fields in conformational-analysis of carbohydrate molecules. Comparison with amber molecular mechanics and dynamics calculations for methyl alpha-lactoside. Int. J. Biol. Macromol. **17**, 137–148 (1995)
31. Allinger, N.L., Yuh, Y.H., Lii, J.H.: Molecular mechanics. The MM3 force field for hydrocarbons. Vibrational frequencies and thermodynamics. J. Am. Chem. Soc. **111**, 8551–8566 (1989)
32. Still, W.C., Tempzyk, A., Hawley, R., Hendrickson, T.: Semianalytical treatment of solvation for molecular mechanics and dynamics. J. Am. Chem. Soc. **112**, 6127–6129 (1990)
33. Poveda, A., Asensio, J.L., Martin-Pastor, M., Jiménez-Barbero, J.: Solution conformation and dynamics of a tetrasaccharide related to the Lewis(x) antigen deduced by NMR relaxation measurements. J. Biomol. NMR **10**, 29–43 (1997)
34. Corzana, F., Cuesta, I., Freire, F., Revuelta, J., Bastida, A., Jiménez-Barbero, J., Asensio, J.L.: The pattern of distribution of amino groups modulates the structure and dynamics of natural aminoglycosides: implications for RNA recognition. J. Am. Chem. Soc. **129**, 2849–2865 (2007)
35. Morris, G.M., Goodsell, D.S., Halliday, R.S., Huey, R., Hart, W. E., Belew, R.K., Olson, A.J.: Automated docking using a Lamarckian genetic algorithm and empirical binding free energy function. J. Comput. Chem. **19**, 1639–1647 (1998)
36. The Protein Data Bank: Berman, H.M., Westbrook, J., Feng, Z., Gilliland, G., Bhat, T.N., Weissig, H., Shindyalov, I.N., Bourne, P.E.: Nucleic Acids Res. **28**, 235–242 (2000). http://www.rcsb.org/pdb
37. Jiménez, M., André, S., Siebert, H.-C., Gabius, H.-J., Solís, D.: AB-type lectin (toxin/agglutinin) from mistletoe: differences in affinity of the two galactoside-binding Trp/Tyr-sites and regulation of their functionality by monomer/dimer equilibrium. Glycobiology **16**, 926–937 (2006)
38. Kajihara, Y., Kamiyama, D., Yamamoto, N., Sakakibara, T., Izumi, M., Hashimoto, H.: Synthesis of 2-[(2-pyridyl)amino] ethyl β-D-lactosaminide and evaluation of its acceptor ability for sialyltransferase: a comparision with 4-methylumbelliferyl and dansyl β-D-lactosaminide. Carbohydr. Res. **339**, 1545–1550 (2004)
39. Sanz, D., Perona, A., Claramunt, R.M., Elguero, J.: Synthesis and spectroscopic properties of Schiff bases derived from 3-hydroxy-4-pyridinecarboxaldehyde. Tetrahedron **61**, 145–154 (2005)
40. Dahmen, J., Frejd, T., Grönberg, G., Lave, T., Magnusson, G., Noori, G.: 2-Bromoethyl glycosides: synthesis and characterisation. Carbohydr. Res. **116**, 303–307 (1983)
41. Pace, V., Martínez, F., Fernández, M., Sinisterra, J.V., Alcántara, A.R.: Effective monoallylation of anilines catalyzed by supported KF. Org. Lett. **9**, 2661–2664 (2007)
42. Gitlin, G., Bayer, E.A., Wilchek, M.: Studies on the biotin-binding site of avidin. Lysine residues involved in the active site. Biochem. J. **242**, 923–926 (1987)
43. Gitlin, G., Bayer, E.A., Wilchek, M.: Studies on the biotin-binding site of avidin. Tryptophan residues involved in the active site. Biochem. J. **250**, 291–294 (1988)
44. Leteux, C., Stoll, M.S., Childs, R.A., Chai, W., Vorozhaikina, M., Feizi, T.: Influence of oligosaccharide presentation on the interactions of carbohydrate sequence-specific antibodies and the selectins. Observations with biotinylated oligosaccharides. J. Immunol. Methods. **227**, 109–119 (1999)
45. Angus, D.I., Kiefel, M.J., von Itzstein, M.: The synthesis of biotinylated carbohydrates as probes for carbohydrate-recognizing proteins. Bioorg. Med. Chem. **8**, 2709–2718 (2000)

46. Fernández-Alonso, M.C., Cañada, F.J., Barbero-Jiménez, J., Cuevas, G.: Molecular recognition of saccharides by proteins. Insights on the origin of the carbohydrate–aromatic interactions. J. Am. Chem. Soc **127**, 7379 –7386 (2005)
47. Gabius, H.-J.: Animal lectins. Eur. J. Biochem. **243**, 543–576 (1997)
48. Lee, R.T., Gabius, H.-J., Lee, Y.C.: Ligand binding characterization of the major mistletoe lectin. J. Biol. Chem. **267**, 23722–23727 (1992)
49. Martin, J.N., Muñoz, E.V., Shwergold, C., Souard, F., Asensio, J. L., Jiménez-Barbero, J., Cañada, J., Vicent, C.: Carbohydrate-based DNA ligands: sugar-oligoamides as a tool to study carbohydrate-nucleic acid interactions. J. Am. Chem. Soc **127**, 9518 –9533 (2005)
50. Heaton, N.J., Bello, P., Herradón, B., del Campo, A., Jiménez-Barbero, J.: NMR Study of Intramolecular Interactions between aromatic groups: Van der Waals, charge-transfer, or quadrupolar interactions? J. Am. Chem. Soc **120**, 9632 –9645 (1998)
51. Bharadwaj, S., Kaltner, H., Korchagina, E.Y., Bovin, N.V., Gabius, H.-J., Surolia, A.: Microcalorimetric indications for ligand binding as a function of the protein for galactoside-specific plant and avian galectins. Biochim. Biophys. Acta **1472**, 191–196 (1999)
52. Espinosa, J.F., Bruix, M., Jarreton, O., Troels Skrydstrup, J.M.B., Jiménez-Barbero, J.: Conformational differences between *C*- and *O*-glycosides: The (-*C*-mannobiose/(-*O*-mannobiose case. Chem. Eur. J **5**, 442–448 (1999)
53. Siebert, H.-C., André, S., Lu, S.Y., Frank, M., Kaltner, H., van Kuik, J.A., Korchagina, E.Y., Bovin, N., Tajkhorshid, E., Kaptein, R., Vliegenthart, J.F.G., von der Lieth, C.-W., Jiménez-Barbero, J., Kopitz, J., Gabius, H.-J.: Unique conformer selection of human growth-regulatory lectin galectin-1 for ganglioside GM1 versus bacterial toxins. Biochemistry **42**, 14762–1473 (2003)
54. Asensio, J.L., Canada, F.J., Garcia-Herrero, A., Murillo, M.T., Fernández-Mayoralas, A., Johns, B.A., Janusz, K., Zhu, Z., Johnson, C.R., Jiménez-Barbero, J.: Conformational behavior of aza-C-glycosides: experimental demonstration of the relative role of the exo-anomeric effect and 1,3-type interactions in controlling the conformation of regular glycosides. J. Am. Chem. Soc **121**, 11318–11329 (1999)
55. Alonso-Plaza, J.M., Canales, M.A., Jimenez, M., Roldan, J.L., Garcia-Herrero, A., Iturrino, L., Asensio, J.L., Canada, F.J., Romero, A., Siebert, H.C., André, S., Solís, D., Gabius, H.-J., Jiménez-Barbero, J.: NMR investigations of protein-carbohydrate interactions: insights into the topology of the bound conformation of a lactose isomer and β-galactosyl xyloses to mistletoe and galectin-1. Biochim. Biophys. Acta **1568**, 225–236 (2001)
56. Danguy, A., Kayser, K., Bovin, N.V., Gabius, H.-J.: The relevance of neoglycoconjugates for histology and pathology. Trends Glycosci. Glycotechnol. **7**, 261–275 (1995)
57. Gabius, H.-J.: Glycohistochemistry: the why and how of detection and localization of endogenous lectins. Anat. Histol. Embryol. **30**, 3–31 (2001)